Journal of the Endocrine Society, 2023, **7**, 1–11
https://doi.org/10.1210/jendso/bvad072
Advance access publication 6 June 2023
Clinical Research Article

Metreleptin Robustly Increases Resting-state Brain Connectivity in Treatment-naïve Female Patients With Lipodystrophy

Haiko Schlögl,[1,2] Arno Villringer,[3,4] Konstanze Miehle,[1] Mathias Fasshauer,[5] Michael Stumvoll,[1,2] and Karsten Mueller[3,6]

[1]Department of Endocrinology, Nephrology, Rheumatology, Division of Endocrinology, University Hospital Leipzig, 04103 Leipzig, Germany
[2]Helmholtz Institute for Metabolic, Obesity and Vascular Research (HI-MAG) of the Helmholtz Zentrum München at the University of Leipzig and University Hospital Leipzig, 04103 Leipzig, Germany
[3]Max-Planck-Institute for Human Cognitive and Brain Sciences, 04103 Leipzig, Germany
[4]Day Clinic of Cognitive Neurology, University of Leipzig, 04103 Leipzig, Germany
[5]Institute of Nutritional Sciences, Justus-Liebig-University, 35392 Giessen, Germany
[6]Department of Neurology, Charles University, First Faculty of Medicine and General University Hospital, 120 00 Prague, Czech Republic

Correspondence: Haiko Schlögl, MD, Department of Endocrinology, Nephrology, Rheumatology, Division of Endocrinology, University Hospital Leipzig, Liebigstr. 20, 04103 Leipzig, Germany. Email: haiko.schloegl@medizin.uni-leipzig.de.

Abstract

Context: Research in lipodystrophy (LD) and its treatment with metreleptin has not only helped patients with LD but has opened new directions in investigating leptin's role in metabolism and the regulation of eating behavior. Previously, in a study with patients with LD undergoing metreleptin treatment using functional magnetic resonance imaging (MRI), we found significantly increased resting-state brain connectivity in 3 brain areas including the hypothalamus.

Objective: In this study, we aimed to reproduce our functional MRI findings in an independent sample and compare results to healthy participants.

Design: Measurements in 4 female patients with LD undergoing metreleptin treatment and 3 healthy untreated controls were performed at 4 different time points over 12 weeks. To identify treatment-related brain connectivity alterations, eigenvector centrality was computed from resting-state functional MRI data for each patient and each session. Thereafter, analysis aimed at detecting consistent brain connectivity changes over time across all patients.

Results: In parallel to metreleptin treatment of the patients with LD, we found a significant brain connectivity increase in the hypothalamus and bilaterally in posterior cingulate gyrus. Using a 3-factorial model, a significant interaction between group and time was found in the hypothalamus.

Conclusions: Investigating brain connectivity alterations with metreleptin treatment using an independent sample of patients with LD, we have reproduced an increase of brain connectivity in hedonic and homeostatic central nervous networks observed previously with metreleptin treatment. These results are an important contribution to ascertain brain leptin action and help build a foundation for further research of central nervous effects of this important metabolic hormone.

Key Words: metreleptin, leptin, lipodystrophy, neuroimaging, brain connectivity, hypothalamus

Abbreviations: BMI, body mass index; EC, eigenvector centrality; HbA1c, hemoglobin A1c; LD, lipodystrophy; MRI, magnetic resonance imaging; SPM, statistical parametric mapping; TE, echo time; TFEQ, *Three factor eating questionnaire*; TR, repetition time; VAS, visual analog scale.

Recent research is aimed at investigating the lipodystrophy (LD) syndrome [1, 2] that is mainly associated with very low leptin levels. Through the development of the recombinant human methionyl leptin (metreleptin) and its approval by the Food and Drug Administration in 2014 [3] and the European Medicines Agency in 2018 [4], there is a causal treatment option of leptin deficiency with its detrimental consequences occurring in LD, like diabetes mellitus, hypertriglyceridemia, atherosclerosis, and cardiovascular disease [1, 5–7]. Research in LD and treatment with metreleptin has not only helped patients with LD, but also opened new directions in research investigating leptin's role, and metreleptin's potential benefit, in other diseases with leptin deficiency, such as anorexia nervosa [8].

Reduced leptin blood concentrations in LD are accompanied by disturbed eating behavior. Affected patients experience strong feelings of hunger and a decreased duration of satiety after eating. However, patients usually do not develop severe obesity, but remain in body mass index (BMI) ranges of 25 to 30 kg/m². Leptin treatment in patients with LD leads to a normalization of eating behavior. Perceived hunger, importance of eating, eating frequencies, and liking ratings of food pictures significantly decrease [9, 10].

Received: 22 July 2022. **Editorial Decision:** 26 May 2023. **Corrected and Typeset:** 3 July 2023

The neural mechanisms behind the effects of leptin on human eating behavior are not yet fully understood. Central nervous system effects of metreleptin were demonstrated [11] in the early days of functional magnetic resonance imaging (MRI). Since then, several other functional MRI studies have been conducted in patients with leptin deficiency particularly investigating congenital leptin deficiency and other specific forms of LD. However, because of the rarity of these diseases, studies on the central nervous effects of metreleptin have had very low case numbers, ranging from 1 to 10 [9, 11–13].

In a previous study, we investigated the effects of metreleptin treatment on resting-state brain connectivity over 52 weeks in leptin-deficient patients with partial and generalized LD [9]. Here, we investigated brain connectivity alterations using a specific network centrality approach, namely eigenvector centrality, obtained from so-called "resting-state" functional MRI. Our study was the first and is, to our knowledge, the only study to date investigating the effects of metreleptin on resting-state brain connectivity in previously leptin-deficient patients [9]. Resting-state connectivity significantly increased over the course of metreleptin treatment in 3 brain areas: the hypothalamus, insula/superior temporal gyrus, and medial prefrontal cortex. Perceived hunger, the importance of eating, eating frequencies, and liking ratings of food pictures significantly decreased during that time. Thus, leptin treatment was accompanied by long-term changes of both hedonic and homeostatic central nervous networks regulating eating behavior, as well as by decreased feelings of hunger and a diminished incentive value of food [9].

Despite being the best noninvasive option we have to investigate acute changes in deep brain areas in humans, such as the hypothalamus, functional MRI is susceptible to false-positive results [13]. Reproducibility [14–16] of functional MRI findings is seen as one of the key indicators for scientifically meaningful results [17], especially in studies with small case numbers like those with rare diseases such as LD, including our own. Another limitation of our previous study was that it lacked a healthy control group and thus the experimental design did not allow the distinction between metreleptin treatment effects and nonspecific order effects.

In this study, we aimed to (1) reproduce our brain connectivity findings in an independent sample using the same connectivity measure of eigenvector centrality using resting-state functional MRI as in our previous study and (2) add healthy participants to control for nonspecific order effects.

Here, in an independent sample of patients with LD undergoing metreleptin treatment, we have reproduced the increase in connectivity in the hypothalamus, the homeostatic center of the brain. These effects were specific to metreleptin treated patients with LD and did not occur in untreated healthy controls.

Materials and Methods

Patients With LD

Four patients with LD (all female) eligible for metreleptin treatment at the University Hospital Leipzig participated in the functional MRI study. Metreleptin treatment was performed following clinical necessity, independently of the functional MRI study. Baseline characteristics and laboratory data of included patients are summarized in Table 1, together with data of healthy controls. Inclusion criteria for leptin treatment were established LD, age ≥5 years, insufficiently controlled diabetes mellitus and/or hypertriglyceridemia despite adequate antihyperglycemic and lipid-lowering medication, respectively. Exclusion criteria included pregnancy or lactation, severe renal insufficiency, active malignant disease, primary hematologic abnormalities, infectious liver disease, HIV infection, and hypersensitivity to *Escherichia coli*-derived proteins. All 4 patients had familial partial LD with mutations in the lamin A/C gene and were metreleptin treatment-naïve and consented to participating in the MRI study. Healthy controls were also all female and selected by matching the age and BMI range of patients with LD, and also consented to all study procedures.

Medication

The leptin analogue metreleptin was used for treatment of patients with LD. Metreleptin was provided by Amylin (San Diego, CA)/Bristol-Myers-Squibb (Munich, Germany)/AstraZeneca (London, UK)/Aegerion Pharmaceuticals (Cambridge, MA), respectively, and applied subcutaneously. Metreleptin was administered once daily at 5 mg independent of body weight, according to the manufacturer's instructions. Healthy controls did not receive drug treatment.

Experimental Design

Experiments were performed between July 2017 and March 2020. The design was chosen to be able to replicate our previous findings [9] in an independent cohort. Behavioral tests and MRI scanning in patients with LD were performed at 4 different timepoints in congruence to previous work [9] (ie, 1 day before start of metreleptin supplementation of the patients group [T0], and after 1 [T1], 4 [T2], and 12 weeks [T3] of metreleptin treatment). Other than in previous work [9], measurements after 26 and 52 weeks of metreleptin treatment could not be performed for all 4 patients (among others, because of travel restrictions during the coronavirus disease 2019 pandemic). In untreated healthy controls, 4 measurements were conducted with the same intervals in between. Procedures at each measurement day for patients with LD and healthy controls were identical: participants were asked to have a light breakfast in the morning and no food after that. They arrived at the institution at approximately 1:30 PM. Questionnaires and behavioral tests were performed as further indicated later. Then, at 2:30 PM, a standard meal consisting of 20% of the daily energy requirements calculated for each participant was consumed. Because leptin physiologically mediates satiety, differences between leptin deficiency and imitated physiological leptin concentrations through metreleptin treatment were expected to be most pronounced in the sated state and, therefore, the mentioned calorie amount was chosen to create a state of moderate satiety. We did not choose a higher percentage of daily energy requirements to avoid both a ceiling effect in extreme fullness and postprandial tiredness during the following functional MRI scan. Before and after the meal, patients filled in visual analog scales (VAS). At approximately 3:30 PM, the MRI scan was performed. In patients with LD, the next morning at 8 AM, a fasting blood sample was taken for assessment of metabolic parameters including fasting triglycerides, hemoglobin A1c (HbA1c), and leptin serum concentrations.

Table 1. Baseline characteristics and laboratory data of the study population

	Phenotype of LD	Mutation	Sex	Age (y)	BMI (kg/m²)	Leptin (µg/L)	HbA1c (% [mmol/mol])	TG (mmol/L)
Patient 1	Partial	LMNA	F	52	28.3	3.4	8.6 (70)	1.5
Patient 2	Partial	LMNA	F	45	25.0	2.3	9.2 (77)	2.8
Patient 3	Partial	LMNA	F	26	21.0	1.3	6.1 (43)	21.1
Patient 4	Partial	LMNA	F	26	33.9	3.9	7.3 (57)	41.5
Contr. 1	none	—	F	57	35.7	58.4[a]	5.4 (36)[a]	4.6[a]
Contr. 2	none	—	F	43	29.8	43.9[a]	5.0 (31)[a]	0.8[a]
Contr. 3	none	—	F	28	24.0	4.5[a]	5.1 (32)[a]	0.5[a]

Reference ranges were for HbA1c < 5.7% (<39 mmol/mol) diabetes mellitus ruled out, 5.7% to 6.4% (39-47 mmol/mol) increased risk for diabetes mellitus, ≥ 6.5% (≥48 mmol/mol) diabetes mellitus and for TG <1.7 mmol/L. Leptin serum concentrations are sex-, age-, and BMI-dependent and correlate with the percentage of body fat [18–2018–20]. In patients with lipodystrophy, leptin concentrations are usually lower than in healthy persons [21].
Abbreviations: BMI, body mass index; Contr., healthy control person; F, female; HbA1c, hemoglobin A1c; LD, lipodystrophy; LMNA, lamin A/C; TG, triglycerides.
[a]Laboratory values in healthy controls were assessed at T3. Between T0 and T3, in healthy controls there was no intervention, body weight changes during that interval were <2 kg (see Table 2).

Questionnaires, Behavioral Tests, and Laboratory Data

Before all other measurements, the German versions of the *Three factor eating questionnaire* (TFEQ [22]; German version: *Fragebogen zum Essverhalten* [23]) and the Inventory of Eating Behavior and Weight Problems (IEG; German version: *Inventar zum Essverhalten und Gewichtsproblemen*) were filled in. Because the German versions refers more to long-term than acute attitudes toward eating and hunger and satiety feelings, the tests were not performed 1 week after initiation of metreleptin treatment because the time interval to the previous measurement would have been too short. The VAS were bars of 100-mm length for assessment of hunger and satiety feelings. The very left at 0 mm indicated no hunger or satiety, the very right at 100 mm indicated extreme hunger or satiety.

Because of the small sample size, in all tables and figures, we are presenting individual data of all participants. In the text, for better legibility, we report mean values ± SD for the 2 groups (patients and healthy controls).

For analyzing behavioral and laboratory data, IBM SPSS 12 rev. 24 was used for implementing a repeated measures ANOVAs including "group" as an additional factor for patients vs controls. Tests were performed to detect potential within-subjects effects over the 4 repeated measurements. Violation for sphericity was taken into account using the Huynh-Feldt correction [24].

MRI Brain Data Acquisition

For each participant, functional brain data were obtained at all timepoints T0, T1, T2, and T3 using functional MRI with a whole-body 3-T MAGNETOM Skyra scanner (Siemens Healthineers, Erlangen, Germany) and a 32-channel head coil and a gradient-echo echo-planar imaging sequence (multiband factor 3). The following parameters were used: 360 whole brain volumes, acquisition matrix = 82 × 82, and slice thickness = 2.5 mm (0.25 mm gap), resulting in a nominal voxel size of 2.488 × 2.488 × 2.75 mm^3. Further imaging parameters were: 60 axial slices, repetition time (TR) = 2000 ms, echo time (TE) = 22 ms, flip angle = 80°, and bandwidth = 1795 Hz/pixel. For all participants, image acquisition was performed without any specific task in the so-called "resting state." Participants were instructed to fixate on a visual white crosshair, remain still and awake, and not think of anything in particular. The total length of the "resting-state" experiment was 12 minutes (360 volumes with TR = 2000 ms).

For registration and normalization purposes, additional T1-weighted images were acquired with a magnetization-prepared rapid gradient-echo sequence with the following parameters: sagittal orientation, 176 slices, TR = 5000 ms, TE = 2.92 ms, TI1 = 700 ms, TI2 = 2500 ms, FA1 = 4°, FA2 = 5°, echo spacing = 6.9 ms, bandwidth = 240 Hz/pixel, field of view = 256 mm, nominal image resolution 1 × 1 × 1 mm^3, GRAPPA acceleration factor 3.

MRI Data Preprocessing

All functional MRI data sets were analyzed using the CONN toolbox rev. 20b [25, 26] and statistical parametric mapping (SPM) 12 rev. 7771 [27] (Wellcome Centre for Human Neuroimaging, University College London, UK) with Matlab 9.12 rev. 2022a (The MathWorks Inc., Natick, MA). Preprocessing was performed using the default SPM pipeline within the CONN toolbox [25] including realignment for motion correction, unwarping of echo-planar imaging images to correct for distortions, slice-time correction, and normalization to the Montreal Neurological Institute space based on the unified segmentation approach [28]. Normalization was performed with the default settings for resampling and interpolation using a destination resolution of 2 × 2 × 2 mm^3. Thereafter, spatial filtering was applied using a Gaussian kernel with 10-mm full width at half maximum. Image preprocessing also included denoising within the CONN toolbox. To correct for nuisance signal fluctuations, a regression analysis was computed using the signal from regions of cerebrospinal fluid (16 regressors), the signal from regions of white matter (16 regressors), as well as the translational and rotational parameters from head movements obtained by SPM 12 (6 regressors), and the effect of the beginning of the resting-state measurement (2 regressors). Preprocessing was finalized using detrending and band-pass filtering with the cutoff frequencies of 0.01 and 0.1 Hz to achieve a baseline correction.

Brain Network Centrality Analysis

To identify treatment-related connectivity changes, eigenvector centrality (EC) mapping [29] was performed using

Table 2. Body mass index, hemoglobin A1c, and fasting triglycerides of lipodystrophy patients over 12 weeks of metreleptin treatment, and available values for healthy controls

	Baseline	1 week	4 weeks	12 weeks	Within-subjects effects
Body mass index (kg/m²)					
Patient 1	28.3	27.8	27.6	28.2	
Patient 2	25.0	24.2	24.8	24.2	
Patient 3	21.0	21.1	21.5	19.5	
Patient 4	33.9	33.3	33.8	33.9	
Mean	27.1	26.6	26.9	26.5	Not significant
SD	5.4	5.2	5.2	6.1	
Contr. 1	35.7	35.9	36.5	36.2	
Contr. 2	29.8	29.9	30.6	30.4	
Contr. 3	24.0	24.1	23.7	23.6	
Mean	29.8	30.0	30.3	30.0	Not significant
SD	5.8	5.9	6.4	6.3	
Hemoglobin A1c (% [mmol/mol])					
Patient 1	8.6 (70.5)	8.2 (66.3)	7.6 (59.0)	6.9 (52.2)	
Patient 2	9.2 (77.4)	9.0 (74.8)	7.8 (61.9)	6.2 (44.3)	
Patient 3	6.1 (43.4)	6.1 (43.3)	5.9 (40.6)	5.6 (37.2)	
Patient 4	7.3 (56.6)	7.3 (56.4)	6.5 (48.0)	6.3 (44.9)	
Mean	7.8 (62.0)	7.7 (60.2)	6.9 (52.4)	6.2 (44.6)	$P = .045$[a]
SD	1.4 (15.1)	1.2 (13.5)	0.9 (9.9)	0.6 (6.2)	
Triglycerides (mmol/L)					
Patient 1	1.5	1.1	1.2	1.5	
Patient 2	2.8	1.8	2.0	3.7	
Patient 3	21.1	6.2	4.7	3.2	
Patient 4	41.5	20.5	11.6	13.8	
Mean	16.7	7.4	4.9	5.6	Not significant
SD	18.8	9.0	4.7	5.6	

Abbreviations: Contr., healthy control participant.
[a]With Huynh-Feldt correction.

the fastECM software [30]. EC provides a measure for detecting central hubs within a brain network using an algorithm similar to Google's PageRank algorithm [31]. For all voxels, a similarity matrix was generated including Pearson correlation coefficients between all functional MRI time courses. To use a similarity matrix with only positive numbers, the value of 1 was added to all correlation values and finally divided by 2 leading to values in the interval [0,1] [30]. Note that according to the theorem of Peron and Frobenius [32], the similarity matrix has a unique real largest eigenvalue, and the corresponding eigenvector has strictly positive components. The EC map was generated using the components of this eigenvector to determine the EC of all voxels, and finally, EC values were normalized resulting in normally distributed centralities.

Within SPM 12, the statistical analysis was performed on the group level using all 16 EC maps for all patients and sessions using the general linear model with a flexible factorial design with factors subject and time. A weighted sum of the parameter estimates was statistically assessed using a *t*-contrast generated by the a priori hypothesis of an increased EC over time (C = [−1 0 1 0]). In addition, we also tested for an EC decrease using the opposite contrast −C. Resulting statistical parametric maps were processed using a voxel-wise threshold of $P < .001$. To take the multiple comparison problem into account, clusters were detected with a minimum size of 80 voxels. To further investigate a potential difference between patients and controls, a flexible factorial model was used with 28 EC maps including the 3 factors of subject, group, and time. Here, a potential interaction between the factors group and time were investigated with an *F*-contrast *diag*(C, −C) using the diagonal matrix with elements C and −C at the main diagonal blocks. The resulting *F*-map was further processed with the same voxel threshold of $P < .001$ as used previously, and significant results were obtained using a minimum cluster size of 80 voxels.

Visualization

Figures showing orthogonal brain sections were generated using Mango v 4.1 (Research Imaging Institute, University of Texas Health Science Center, San Antonio) with the "Build

Surface" option and the "Cut Plane" feature. Statistical parametric maps were imported using the "Add Overlay" function. Bar plots were obtained from SPM12 and plotted with Matlab.

Results

Anthropometric and Metabolic Parameters

Baseline characteristics at T0 of all patients and untreated healthy controls are summarized in Table 1. Patients with LD were 26 to 52 years old; BMI range was 21.0 to 33.9 kg/m². Baseline leptin serum concentrations ranged from 1.3 to 3.9 µg/L, HbA1c from 6.1% to 9.2%, and serum triglyceride concentrations from 1.5 to 41.5 mmol/L. Healthy controls were 28 to 57 years old; BMI range was 24.0 to 35.7 kg/m². Laboratory values in healthy controls were only measured at T3. Leptin serum concentrations in control participants ranged from 4.5 to 58.4 µg/L, HbA1c from 5.0% to 5.4%, and serum triglyceride concentrations from 0.5 to 4.6 mmol/L. As in our larger previous study [9], in patients with LD, metreleptin treatment numerically led to a mild decrease in BMI (no significant within-subjects effects), improvements in HbA1c (significant within-subjects effects; $P = .045$ with Huynh-Feldt correction), and numerically a decrease in fasting triglycerides (no significant within-subjects effects, Table 2). Between T0 and T3, in healthy controls, there was no intervention; body weight changes during that interval were <2 kg (Table 2).

Visual Analog Scales for Hunger and Satiety 90 Minutes After the Standard Meal

Data from VAS for hunger 90 minutes after the standard meal on the 0 to 100 mm scale on individual level are presented in Fig. 1. In patients with LD, mean ± SD hunger at baseline (T0) was 42 ± 37 mm, 4 ± 7 mm after 1 week (T1), 7 ± 9 mm after 4 weeks (T2), and 6 ± 10 mm after 12 weeks (T3) of metreleptin treatment (Fig. 1). Satiety scores were 45 ± 43 mm at T0, 82 ± 29 mm at T1, 83 ± 12 mm at T2, and 86 ± 22 mm at T3 (not depicted). In healthy controls, mean hunger scores from T0 to T3 were 5 ± 6 mm, 26 ± 38 mm, 33 ± 25 mm, and 23 ± 26 mm (Fig. 1). Mean satiety scores were 73 ± 12 mm, 59 ± 36 mm, 53 ± 24 mm, and 49 ± 26 mm (not depicted). A 2-factorial model including the factors time (T0; T1; T2; T3) and group (patients; controls) showed a significant time*group interaction ($P = .031$ with Huynh-Feldt correction).

Eating Behavior Questionnaires

Factors 2 ("Disinhibition") and 3 ("Hunger") of the TFEQ were the 2 factors with significant reduction through metreleptin treatment in [9]. In this study, in patients with LD mean scores ± SD for "Disinhibition" were at T0, T2, and T3 (no assessment at T1) 11 ± 4, 7 ± 3, and 5 ± 3 and for "Hunger" 11 ± 3, 4 ± 3, and 3 ± 4. In healthy control persons, scores for "Disinhibition" were 8 ± 5, 8 ± 6, and 7 ± 7 (no significant result) and for "Hunger" 7 ± 1, 6 ± 2, and 5 ± 0 (significant time*group interaction; $P = .019$ with Huynh-Feldt correction). All individual scores for all 3 factors of the TFEQ and all individual scores for the scales of the IEG with significant reductions through metreleptin treatment in previous work [9] (scales: 1, importance of eating; 2, strength and triggering of desire to eat; 7, cognitive restraint of eating; 9, attitude toward obese persons; and 11, eating between meals) are presented in Fig. 2 (TFEQ) and Supplementary Fig. S1 [33] (IEG).

Brain Connectivity Alterations

Using resting-state functional MRI and EC mapping, a significant increase of brain connectivity was detected over the course of metreleptin treatment. Using the contrast vector C, a significant EC increase was found in the hypothalamus (voxel-level $P < .001$, cluster-level $P = .006$, cluster size $k_E = 160$, cluster maximum at [−6 8 −14], $T = 11.96$, $Z = 4.94$) (Fig. 3A). The fitted EC values for the coordinate [−6 8 −14] are shown in Fig. 3C. In addition, two further clusters were found in the posterior cingulate gyrus (left: voxel-level $P < .001$, cluster-level $P = .007$, cluster size $k_E = 151$, cluster maximum at [−14 −62 28], $T = 10.84$, $Z = 4.77$; right: voxel-level $P < .001$, cluster-level $P = .007$, cluster size $k_E = 155$, cluster maximum at [12 −60 32], $T = 9.71$, $Z = 4.58$) (Fig. 4). No significant result was obtained with the inverse contrast −C (ie, no EC decrease was observed).

Using the 3-factorial model including the factors subject, group, and time, a significant interaction between group and time was found in the hypothalamus (voxel-level $P < .001$, cluster-level $P = .020$, cluster size $k_E = 94$, cluster maximum at [−4 6 −14], $F = 27.99$, $Z = 4.30$), but in no other brain region (Fig. 3B). Thus, a significant brain connectivity difference between patients and controls was only obtained for the hypothalamus.

To demonstrate consistency between our current hypothalamus result and our previous findings [9], we displayed the previous findings together with the result of our current data (Fig. 5). For this purpose, we extracted the resulting statistical parametric map from our previous study [9] and processed this parametric map with the same visualization technique as used in the current study. Finally, as an example, we also show the individual normalized EC values for patient 1 for all 4 timepoints over 12 weeks of metreleptin treatment. Supplementary Fig. S2 [33] depicts color-coded EC values of patient 1 for all significant voxels obtained by the statistical analysis (see Fig. 3A).

Discussion

In the current study, we reproduced an increase in hypothalamic connectivity in an independent sample of patients with LD in the first 12 weeks of metreleptin treatment that we have observed in our previous work [9]. This is particularly important given the susceptibility of functional MRI to false positives and the inherently small sample sizes in studies of rare disorders. Thus, our study first replicates functional MRI findings of leptin brain action, which is especially important given the fact that functional MRI is prone to produce false-positive results particularly when investigating a small number of participants. Notably, we found brain connectivity increase not only the hypothalamus, but also in the posterior cingulate gyrus giving a picture of developing of brain dysfunction in LD.

Using "resting-state" functional MRI, the brain connectivity approach of EC attributes a centrality value to each pixel (also called *voxel* in 3 dimensions) of the functional brain image. A voxel receives a large value if it is strongly correlated

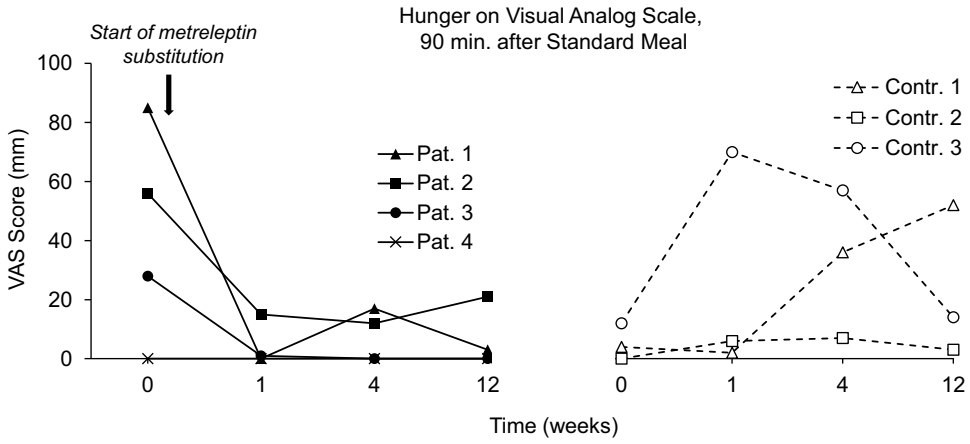

Figure 1. Individual ratings for hunger on visual analog scales, 90 minutes after the standardized meal. Score range was from 0 (no hunger) to 100 mm (extreme hunger). (Left) Lipodystrophy patients (Pat.). (Right) Healthy controls (Contr.). VAS, visual analog scale.

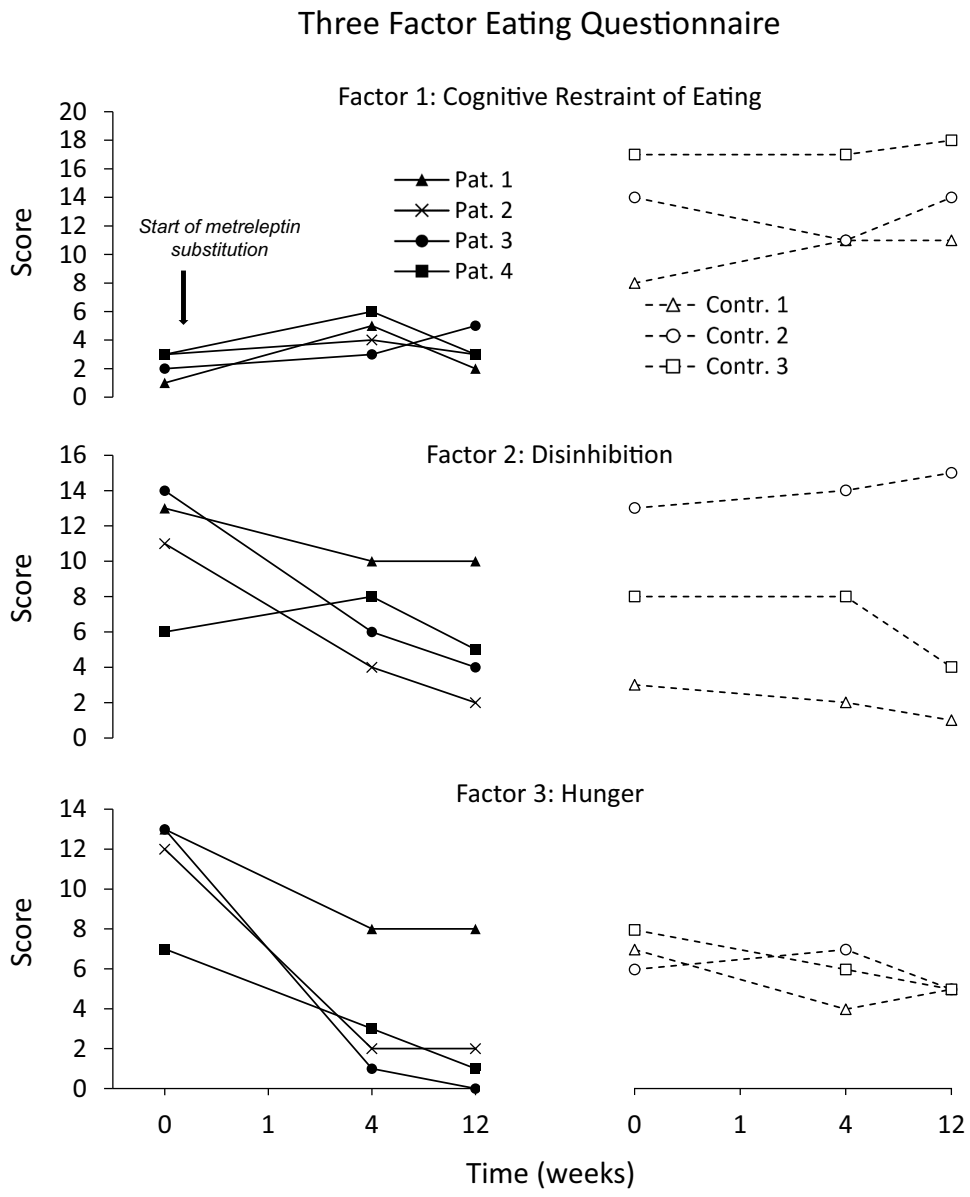

Figure 2. Individual scores for the scales of the 3-factor eating questionnaire. (Left) Lipodystrophy patients (Pat.). (Right) Healthy controls (Contr.). The questionnaire was not filled in 1 week after initiation of metreleptin treatment.

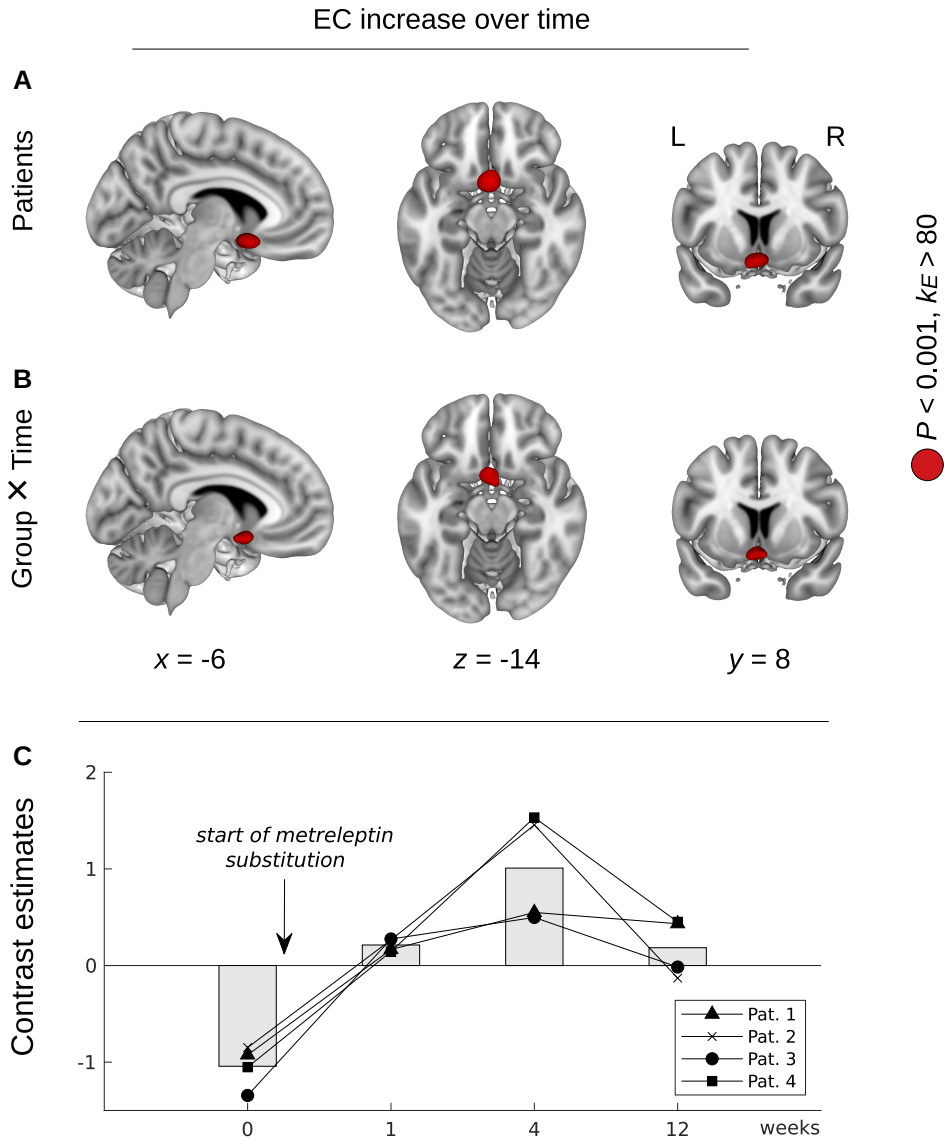

Figure 3. Metreleptin-associated brain connectivity increase detected with functional MRI showing an eigenvector centrality (EC) increase using the contrast C = [−1 0 1 0] (**A**) for patients with lipodystrophy (N = 4) over 12 weeks of metreleptin treatment, (**B**) the 3-factorial model including the factors subject, group (4 patients vs 3 heathy controls), and time (4 repeated measurements for each participant) using the *F*-contrast *diag*(C, −C), and (**C**) contrast estimates at coordinate [−6 8 −14] (hypothalamus) for 4 individual patients (lines) and patient group averages (bars) for all 4 measured timepoints. MRI, magnetic resonance imaging; Pat., patient; k_E, minimum cluster size; L, left; R, right; x, y, z, coordinates in mm.

with many other voxels, which are themselves highly correlated within the network. Google's PageRank algorithm is a variant of eigenvector centrality [29]. The output of the EC analysis is a brain connectivity map showing the major hubs within the network. An increase in connectivity in the homeostatic center of the brain, the hypothalamus, over the 12 weeks of metreleptin treatment, may suggest that metreleptin treatment restored homeostatic satiety signaling via the hypothalamus in our patients.

Indeed, increases in connectivity were again accompanied by decreases—on an individual level—of the majority of measurements of self-reported postprandial hunger feelings. We observed statistically significant decreases of VAS hunger ratings providing a measure for homeostatic hunger in metreleptin treated patients with LD compared with untreated healthy controls. Furthermore, the score of the TFEQ scale "hunger" decreased significantly in patients with LD. This fits well with obtained behavioral data from the larger cohort of our previous study [9]. In that work, we also obtained a significant decrease of hunger feelings during metreleptin treatment that is in line with the observations of others [34]. Note that the statistical analyses were performed with a very small sample and significant values were obtained because of a high degree of intersubject consistency (see Figs. 1 and 2); thus, the interpretation in this cohort is limited. Our current findings strengthen the hypothesis of Schlögl et al [9], that metreleptin, in leptin-deficient patients with LD, restores the response to satiety signals from the body via the hypothalamus. These results are an important contribution to ascertain brain leptin action and provide a foundation for further research of central nervous effects of this important metabolic hormone.

In addition to our brain connectivity findings with the hypothalamus, we also found an increase of EC in the posterior

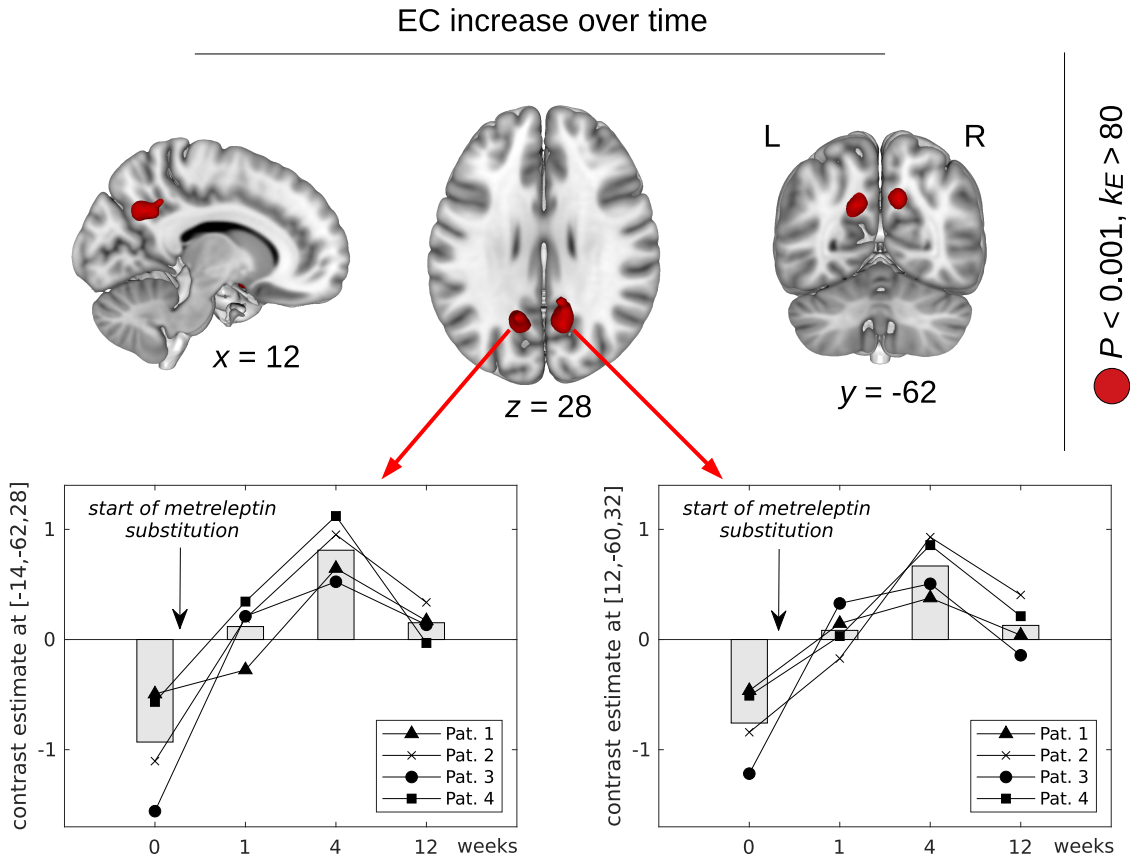

Figure 4. Metreleptin-associated brain connectivity increase detected with functional MRI showing an eigenvector centrality (EC) increase using the contrast C = [−1 0 1 0] for lipodystrophy patients (N = 4) over 12 weeks of metreleptin treatment (top). Contrast estimates are shown at coordinate [−14 −62 28] (left dorsal posterior cingulate gyrus) and [12 −60 32] (right dorsal posterior cingulate gyrus) for the 4 individual patients (lines) and patient group averages (bars) for all 4 measured timepoints (bottom). Pat., patient; k_E, minimum cluster size; L, left; MRI, magnetic resonance imaging; R, right; x, y, z, coordinates in mm.

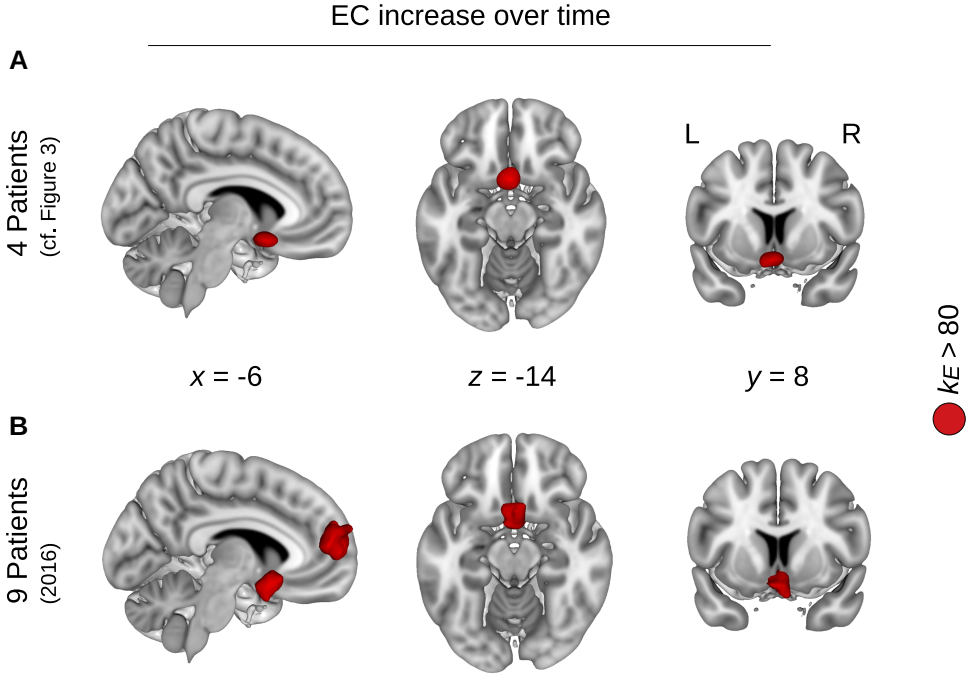

Figure 5. Orthogonal brain sections showing an eigenvector centrality (EC) increase with metreleptin treatment for patients with lipodystrophy (LD) of our current study (top row; see also Fig. 3A) together with an EC increase in our preceding study [9] including 9 patients with LD (independent of the current cohort) during 52 weeks of metreleptin treatment (bottom row). kE, minimum cluster size; L, left; R, right; x, y, z, coordinates in mm.

cingulate gyrus. The posterior cingulate gyrus is a brain region that is part of the limbic system and has connections with the thalamus, also linking it to the hypothalamus [35]. With neuroimaging, food-specific alterations of posterior cingulate gyrus activity have been reported. For example, in a functional MRI study using an event-related design, when watching food pictures, posterior cingulate gyrus activity was higher than when watching nonfood pictures [36]. In another study, using electroencephalography, participants were asked to rate pictures depicting foods in different portion sizes, for example, if they were too small, suitable, or too big for their next meal. Among others, the mid-posterior cingulate and superior temporal gyri showed greater neural source activity for suitable vs nonsuitable meal sizes [37]. This suggests a possible role in the control and evaluation of eating behavior and hunger/satiety signals. The increase in EC we found in posterior cingulate gyrus, coupled with the insula/superior temporal gyrus region that was found in our previous study [9], suggest an involvement of these brain structures in the alterations in eating behavior we found in our patients. In particular, the observed decrease in disinhibition of eating behavior could go together with an increase in willful control of the drive to eat and a more deliberate evaluation of hunger signals and thoughts about food. These signals may be processed in the central nervous regions we found to have increased EC through metreleptin treatment.

In contrast to our previous study, the current study also included healthy control participants that were not undergoing metreleptin treatment, but they were measured at exactly the same 4 timepoints as the patients with LD. Importantly, the brain connectivity increase found in the metreleptin-treated patients with LD did not occur in untreated healthy controls.

However, some limitations of our study must be discussed. First, our control participants were not treated as our patients with LD, but rather serve as a group of healthy controls who did not receive any kind of treatment. This led to several differences between patients with LD and healthy untreated controls, including, among others, the exposure to medical care and treatment by physicians. Moreover, with the control participants, all study assessments were performed by the same physician as assessments in the LD cohort. A placebo-treated LD cohort was not possible because of ethical considerations because the health benefits of the treatment are well documented and metreleptin therapy in LD is the established therapy in patients fulfilling the criteria.

Second, the sample size of the current and the previous study [9] is very small for a typical functional MRI study. However, because LD is very rare, all published functional MRI studies with leptin-deficient patients treated with metreleptin are small, ranging from N = 1 to 10 [9, 11–13]. Nevertheless, studies were able to detect significant effects of metreleptin therapy, including ours, presumably because of the strong effects of substitution of a hormone with such important functions on metabolism and cognition like leptin. Although spurious findings are quite likely in studies with a small sample size, consistent strong effects across studies would suggest, in the present case, that the results are meaningful. Such strong effects are also seen in other metabolic hormones, such as insulin. In the treatment of patients with absolute insulin deficiency in type 1 diabetes, many of the effects of insulin substitution are also well documentable in small cohorts, and even in single patients. Notably, increases in connectivity in the hypothalamus and posterior cingulate gyrus were found in all of our measured patients and with very similar courses over time (see Figs. 3C and 4). Furthermore, because we performed 4 measurements in each patient, the total number of data sets that were included into our model was N = 16, together with the measurements of the control participants, the total number of data sets included into the interaction model was N = 28. Thus, we are confident that, despite a small number of participants, we obtained robust and resilient results. This assumption is strengthened by the fact that our results were specific for the patients with LD patients and replicated our former results of a larger sample.

Third, the study duration was quite short at 12 weeks of observations. Nevertheless, our previous study, which assessed functional brain connectivity over 52 weeks, showed very similar results. This suggests that observed changes in brain connectivity may already be occurring in the first 12 weeks and persist during the further course of metreleptin treatment. Also, the time course of observed changes in behavioral data supports this assumption [9].

Fourth, in this study, we only included women because during the time of the study we could only recruit women who were eligible for metreleptin treatment. This may be due to the more noticeable symptoms of LD in women compared with men. Women with LD seem to be more often diagnosed than men [38] possibly because the typical stature of LD patients (prominent shoulders) is more easily recognized and because of the symptom of amenorrhea. Furthermore, metabolic symptoms in affected female patients seem to be more pronounced than in male patients [39]. Ultimately, the results from the present study cannot be generalized to men.

Finally, we cannot fully exclude that changes in sex hormones during the menstrual cycle of women had an influence on observed changes in brain connectivity [40, 41]. Menstrual cycling was irregular in patient 1 (perimenopausal at time of study) with only 1 menstruation in about 6 months, and in patients 3 and 4 (because of polycystic ovary syndrome). In patient 2 (history of hysterectomy because of myoma), menstrual cycling was no longer observable. None of the patients were taking contraceptives. The stage of the cycle was not taken into account when setting the date of the MRI session in neither the LD patients nor the healthy controls, which should be considered in future studies. However, in our previous study with 9 women [9], intra-individual variations in sex hormone concentrations were only suspected in 2 patients, and results were very similar as in our current study.

Taken together, here we replicate our findings of Schlögl et al [9] in an independent sample of patients with LD. This strengthens our previous findings that metreleptin treatment causes changes of homeostatic central nervous networks regulating eating behavior, which are accompanied by decreased hunger feelings. Via these mechanisms, metreleptin treatment in LD seems to restore physiological mechanisms that are important for the development of satiety. In addition to our findings with metabolic parameters and hunger ratings, for the first time, we were able to replicate findings of leptin effects on functional brain connectivity using resting-state functional MRI in an independent sample. This reinforces the notion that the effects of peripheral hormones on specific central nervous networks can be studied and robustly demonstrated using functional MRI.

Acknowledgments

The authors thank all participants for their partaking in the study and particularly thank Bonnie O`Malley and Joshua Grant for their valuable suggestions with language and style of the manuscript.

Funding

This work was supported by the Federal Ministry of Education and Research (BMBF), Germany, FKZ: 01EO1501 (IFB Adiposity Diseases, project K6a-87 to M.F.); by the Deutsche Forschungsgemeinschaft (DFG; SFB 1052/2, A01 to A.V. and M.S., and C06 to M.F.); and by the Deutsches Zentrum für Diabetesforschung (DZD; grant no. 82DZD00601).

Author Contributions

H.S.: Conceptualization, data curation, formal analysis, investigation. methodology, project administration, validation, visualization, writing—original draft, and writing—review & Editing. A.V.: Funding acquisition and resources. K. Miehle: Writing—review & editing. M.F.: Conceptualization, funding acquisition, supervision, and writing—review & editing. M.S.: Funding acquisition, resources, and writing—review & editing. K. Müller: Conceptualization, data curation, formal analysis, methodology, software, validation, visualization, writing—original draft, and writing—review & editing.

Disclosures

K. Mv has consulted for Aegerion Pharmaceuticals. The other authors have nothing to disclose.

Data Availability

Restrictions apply to the availability of some or all data generated or analyzed during this study to preserve patient confidentiality. The corresponding author will on request detail the restrictions and any conditions under which access to some data may be provided.

Statement of Ethics

The work described in this article has been carried out in accordance with The Code of Ethics of the World Medical Association (Declaration of Helsinki). The Ethics Committee of the University of Leipzig approved this research project according to the national research ethics regulations. All participants, both patients with LD and control persons, gave their written consent for all study procedures. The trial is registered as trial No. 147/10-ek at the ethics committee of the University of Leipzig and at the State Directorate of Saxony (Landesdirektion Sachsen).

References

1. Chevalier B, Lemaitre M, Leguier L, *et al.* Metreleptin treatment of non-HIV lipodystrophy syndromes. *Presse Med*. 2021;50(3):104070.
2. Knebel B, Müller-Wieland D, Kotzka J. Lipodystrophies-disorders of the fatty tissue. *Int J Mol Sci*. 2020;21(22):E8778.
3. FDA. Summary review for regulatory action; Myalept; application number 125390Orig1s000, Ed. C.F.D.E.A. Research. 2014. Accessed May 7, 2022. www.accessdata.fda.gov/drugsatfda_docs/label/2014/125390s000lbl.pdf
4. EMA. Myalepta product information. 2018. Accessed May 7, 2022. www.ema.europa.eu/en/documents/assessment-report/myalepta-epar-public-assessment-report_en.pdf
5. Cook K, Ali O, Akinci B, *et al.* Effect of leptin therapy on survival in generalized and partial lipodystrophy: a matched cohort analysis. *J Clin Endocrinol Metab*. 2021;106(8):e2953-e2967.
6. Oral EA, Gorden P, Cochran E, *et al.* Long-term effectiveness and safety of metreleptin in the treatment of patients with partial lipodystrophy. *Endocrine*. 2019;64(3):500-511.
7. Brown RJ, Oral EA, Cochran E, *et al.* Long-term effectiveness and safety of metreleptin in the treatment of patients with generalized lipodystrophy. *Endocrine*. 2018;60(3):479-489.
8. Hebebrand J, Milos G, Wabitsch M, *et al.* Clinical trials required to assess potential benefits and side effects of treatment of patients with anorexia nervosa with recombinant human leptin. *Front Psychol*. 2019;10:769.
9. Schlögl H, Müller K, Horstmann A, *et al.* Leptin substitution in patients with lipodystrophy: neural correlates for long-term success in the normalization of eating behavior. *Diabetes*. 2016;65(8):2179-2186.
10. Püschel J, Miehle K, Müller K, *et al.* Beneficial effects of leptin substitution on impaired eating behavior in lipodystrophy are sustained beyond 150 weeks of treatment. *Cytokine*. 2019;113:400-404.
11. Farooqi IS, Bullmore E, Keogh J, Gillard J, O'Rahilly S, Fletcher PC. Leptin regulates striatal regions and human eating behavior. *Science*. 2007;317(5843):1355.
12. Frank S, Heni M, Moss A, *et al.* Long-term stabilization effects of leptin on brain functions in a leptin-deficient patient. *PLoS One*. 2013;8(6):e65893.
13. Botvinik-Nezer R, Holzmeister F, Camerer CF, *et al.* Variability in the analysis of a single neuroimaging dataset by many teams. *Nature*. 2020;582(7810):84-88. doi:10.1038/s41586-020-2314-9
14. Schmidt S. Shall we really do it again? The powerful concept of replication is neglected in the social sciences. *Rev Gen Psychol*. 2009;13(2):90-100.
15. Camerer CF, Dreber A, Holzmeister F, *et al.* Evaluating the replicability of social science experiments in nature and science between 2010 and 2015. *Nat Hum Behav*. 2018;2(9):637-644.
16. Nosek BA, Errington TM. What is replication? *PLoS Biol*. 2020;18(3):e3000691.
17. Poldrack RA, Baker CI, Durnez J, *et al.* Scanning the horizon: towards transparent and reproducible neuroimaging research. *Nat Rev Neurosci*. 2017;18(2):115-126.
18. Considine RV, Sinha MK, Heiman ML, *et al.* Serum immunoreactive-leptin concentrations in normal-weight and obese humans. *N Engl J Med*. 1996;334(5):292-295.
19. Zhou X, Chai Y, Chen K, Yang Y, Liu Z. A meta-analysis of reference values of leptin concentration in healthy postmenopausal women. *PLoS One*. 2013;8(8):e72734.
20. Isidori AM, Strollo F, Morè M, *et al.* Leptin and aging: correlation with endocrine changes in male and female healthy adult populations of different body weights. *J Clin Endocrinol Metab*. 2000;85(5):1954-1962.
21. Haque WA, Shimomura I, Matsuzawa Y, Garg A. Serum adiponectin and leptin levels in patients with lipodystrophies. *J Clin Endocrinol Metab*. 2002;87(5):2395.
22. Stunkard AJ, Messick S. The three-factor eating questionnaire to measure dietary restraint, disinhibition and hunger. *J Psychosom Res*. 1985;29(1):71-83.
23. Pudel V, Westhöfer J. *Fragebogen Zum Ebverhalten (FEV)*. Hogrefe Verlag; 1989.
24. Huynh H, Feldt LS. Estimation of the box correction for degrees of freedom from sample data in randomized block and split-plot designs. *J Educ Stat*. 1976;1(1):69.

25. Whitfield-Gabrieli S, Nieto-Castanon A. Conn: a functional connectivity toolbox for correlated and anticorrelated brain networks. *Brain Connect*. 2012;2(3):125-141.
26. Nieto-Castanon A. *Handbook of Functional Connectivity Magnetic Resonance Imaging Methods in CONN*. Hilbert Press; 2020.
27. Friston KJ, Ashburner JT, Kiebel SJ, Nichols TE, Penny WD. *Statistical Parametric Mapping: The Analysis of Functional Brain Images*. Academic Press, Elsevier; 2006.
28. Ashburner J, Friston KJ. Unified segmentation. *NeuroImage*. 2005;26(3):839-851.
29. Lohmann G, Margulies DS, Horstmann A, *et al*. Eigenvector centrality mapping for analyzing connectivity patterns in fMRI data of the human brain. *PLoS One*. 2010;5(4):e10232.
30. Wink AM, de Munck JC, van der Werf YD, van den Heuvel OA, Barkhof F. Fast eigenvector centrality mapping of voxel-wise connectivity in functional magnetic resonance imaging: implementation, validation, and interpretation. *Brain Connect*. 2012;2(5):265-274.
31. Brin S, Page L. Reprint of: the anatomy of a large-scale hypertextual web search engine. *Comput Netw*. 2012;56(18):3825-3833.
32. Frobenius G. Über Matrizen aus nicht negativen Elementen. 1912;23:456-477.
33. Schlögl H, Villringer A, Miehle K, Fasshauer M, Stumvoll M, Mueller K. Data from: metreleptin robustly increases resting-state brain connectivity in treatment-naïve female patients with lipodystrophy. Generic digital repository. Date of deposit 22 June 2023. https://doi.org/10.5281/zenodo.8071392
34. McDuffie JR, Riggs PA, Calis KA, *et al*. Effects of exogenous leptin on satiety and satiation in patients with lipodystrophy and leptin insufficiency. *J Clin Endocrinol Metab*. 2004;89(9):4258-4263.
35. Risold P, Thompson R, Swanson L. The structural organization of connections between hypothalamus and cerebral cortex. *Brain Res Rev*. 1997;24(2-3):197-254.
36. Charbonnier L, van der Laan LN, Viergever MA, Smeets PAM. Functional MRI of challenging food choices: forced choice between equally liked high- and low-calorie foods in the absence of hunger. *PLoS One*. 2015;10(7):e0131727.
37. Toepel U, Bielser M-L, Forde C, *et al*. Brain dynamics of meal size selection in humans. *NeuroImage*. 2015;113:133-142.
38. Hussain I, Garg A. Lipodystrophy syndromes. *Endocrinol Metab Clin North Am*. 2016;45(4):783-797.
39. Garg A. Gender differences in the prevalence of metabolic complications in familial partial lipodystrophy (Dunnigan variety). *J Clin Endocrinol Metab*. 2000;85(5):1776-1782.
40. Arélin K, Mueller K, Barth C, *et al*. Progesterone mediates brain functional connectivity changes during the menstrual cycle-a pilot resting state MRI study. *Front Neurosci*. 2015;9:44.
41. Hidalgo-Lopez E, Mueller K, Harris T, Aichhorn M, Sacher J, Pletzer B. Human menstrual cycle variation in subcortical functional brain connectivity: a multimodal analysis approach. *Brain Struct Funct*. 2020;225(2):591-605.